

A QUICK-TEST METHOD BASED ON ACOUSTIC EMISSION FOR THE IN-PROCESS CHARACTERIZATION OF CONVENTIONAL GRINDING WHEELS

M. Eng. ADRIANO BOARON

Laboratório de Mecânica de Precisão (LMP), Federal University of Santa Catarina (UFSC),
Brazil

PROF. DR.-ING. WALTER LIINDOLFO WEINGAERTNER

Laboratório de Mecânica de Precisão (LMP), Federal University of Santa Catarina (UFSC),
Brazil

PROF. DR. H. C. DR.-ING. ECKART UHLMANN

Institut für Werkzeugmaschinen und Fabrikbetrieb (IWF), Technische Universität Berlin,
Germany

ABSTRACT

A quick-test method for the in-process characterization of a conventional grinding wheel is proposed based on the acoustic emission technology. For implementing the method, a specific experimental rig and a particular software application have been developed. Both the experimental rig and the software application permit to recognize interferences between the grinding wheel and a dressing tool in a range of 1 μm . The acquired AE_{RAW} signals derived from such interferences (elastic deformation range) are used as input data for a specific developed signal processing technique, which allows extracting in-process quantified information from the grinding wheel's topography features. The quantified information associated with the grinding wheel's topography is based on both a time domain and a frequency domain in-process analysis. The quick-test method is validated by correlating the obtained quantified information from the grinding wheel's topography with both the post-process measurement of the grinding force, (components F_t and F_n) and the post-process measurements of the effective roughness of the grinding wheel (parameter R_{ts}).

Index Terms – Cylindrical External Plunge Grinding, Grinding Wheel Topography, Process Monitoring, Acoustic Emission

1. INTRODUCTION

In the context of today's globalized and competitive manufacturing industry, the trend towards a sustainable and effective production requires constant process optimization. Therefore, technical and innovative solutions which permit both a better use of the available resources and product quality are unremittingly in evidence. Among the wide range of industrial process, the grinding process is used when parts with close tolerances and high surface quality are demanded.

Nowadays, a main research subject in the grinding process which claims special attention consists in properly evaluating the grinding wheel's topography during the grinding process. The main goal of the current research consists in developing and validating a dynamic in-process method for determining the topographic characteristics of a conventional grinding wheel.

The proposed method is based on both a specific experimental rig and an AE-based procedure, which employs an instrumented diamond tip, a particular hardware and a

developed software. The in-process evaluation of the grinding wheel's topography is then carried out by moving the instrumented diamond tip along the effective width of the grinding wheel under interferences of 1 μm , thus without removing abrasive grains from the surface of the grinding wheel (elastic deformation range). The relative movement amid the grinding wheel and the diamond tip under such contact interferences originates broadband spectrum of AE events, which are detected by the AE transducer and converted to an electric tension, as an AE_{RAW} time-dependent signal. The AE_{RAW} signals are simultaneously transferred to an appropriately hardware, aiming at the on-line conditioning and sampling of the original AE_{RAW} signals without aliasing effect. Based on the sampled AE_{RAW} signals, a software application has been developed, in order to allow extracting in-process quantified information about the grinding wheel's topography. The quantitative information about the grinding wheel's topography obtained with this procedure is firstly based on in-process time domain analysis, by using a specific signal conditioning technique. Additionally, it is also possible to conduct in-process frequency domain analysis with the aim of obtaining complementary information about the topography of the grinding wheel. During the experiments, the main factors which present direct influence on the time domain quantified information were varied into distinct levels, in order to define an optimized experimental condition to characterizing the grinding wheel's topography.

The possibility to use the proposed quick-test method to extract in-process quantified information from the grinding wheel's topography features (without interrupting the grinding process and changing the experimental setup for a post-analysis) is the first main advantage of such procedure. Besides, in comparison with other grinding wheel's characterization methods proposed in the literature, the present method also permits to achieve in-process information related to the topography of the grinding wheel, by using common and real grinding wheel velocities which are usually employed in the industrial praxis (for example, $v_s = 30 \text{ m/s}$), with no need to decelerate the grinding wheel and then representing a more feasible information related to the grinding process. The validation of the proposed dynamic in-process method is carry out by correlating the obtained quantified information with both the post-process measurement of the grinding force, (components F_t and F_n) and the post-process measurements of the effective roughness of the grinding wheel (parameter R_{ts}), after grinding specimens without spark-out time, with a predefined specific material removal, V'_w .

2. ACOUSTIC EMISSION IN GRINDING

Acoustic emission (AE) can be understood as a class of phenomena, in which transient elastic waves are generated by the rapid release of energy from local sources in the material. Also called sometimes as "structure-born sound", AE typically refers to the elastic wave propagation in the ultrasonic frequency range domain (about 20 kHz up to 2000 kHz), [1], [2], [10].

When a material is deformed by some kind of external stimulus, as occurs on grinding operations (contact and friction between grits and workpiece) the lattice structure of the material is distorted and rearranged. This process provides enough energy to generate tension waves (Rayleigh waves) on layers situated near the origin. This waves travel in a solid, liquid and gas and can be detected by a suitable AE transducer [3].

The grinding process is characterized by the randomly contact of a large amount of cutting edges on the surface of the workpiece. All the individual contacts that are caused by the grits can be considered as a source of pulse deformation or stress on the workpiece. During the grinding process, as the grains wear increases with time, the individual characteristics of the wheel also change, leading to different cutting edges and grain distributions on the grinding wheel [4].

The sources of AE in the grinding process are mainly the bond and grain fracture, grain cracks and friction between abrasive grain and workpiece, all of them directly connected to the chip formation process (Hundt *apud* [5]), and wheel wear. Figure 1 exemplifies the major sources of AE that can be found in grinding.

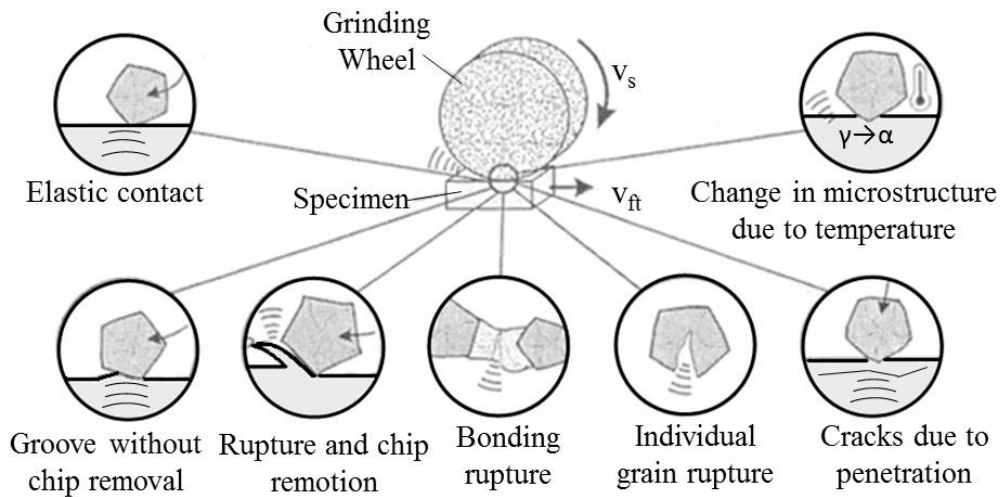


Figure 1: Sources of acoustic emission in grinding. Adapted and based on [6].

3. GRINDING WHEEL TOPOGRAPHY

The topography of a grinding wheel is associated with the definition and mapping of the grinding wheel's shape and its peripheral surface. Both the macrotopography and microtopography are important although in different ways. The basic wheel shape is part of the macrotopography and is important for the overall accuracy of the manufactured workpiece's profile. Microtopography is also significant for maintaining the required workpiece's profile, but additionally for the workpiece's quality and energy requirements in grinding [7].

The basic macrotopographic aspects associated with the grinding wheel can be resumed as the diameter deviation Δ_r , the radial run-out E_s , and the ovality O_s . The sum of these macrotopographic aspects leads to the overall waviness W_s in grinding wheels, Figure 2-a [8].

The microtopographic characteristics are defined by the shape of the cutting edges and are directly influenced by the grinding wheel's wear which conducts to the flattening and breakage of the grains, as well as to the loading of the grinding wheel and the grain's drop-out, Figure 2-b. The microtopography plays an important role on the workpiece's profile, workpiece's roughness and on the energy requirements. The changes in the microtopography influence the down-time for redressing, wheel life and removal rates [7].

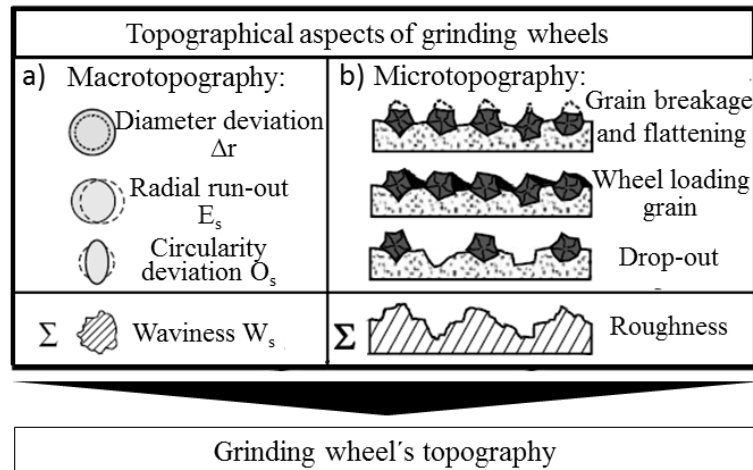


Figure 2: Topographical characteristics of grinding wheels. Adapted and based on [8].

4. METHODS FOR DETERMINING THE GRINDING WHEEL'S TOPOGRAPY

Among the diverse existing methods for determining the grinding wheel's topography three basic methods are currently used: a) static methods, b) dynamic methods, and c) kinematic methods, [Bruecher 1996] apud [3], [8]. In the static methods, the measurement of the grinding wheel's topography is carry out either without moving the grinding wheel, or by displacing it very slowly. All abrasive grains on the surface of the grinding tool are considered. This method does not take the kinematics of the grinding process into account.

On the other hand, in the dynamic methods the number of the actual abrasive grains engagements is measured. The active cutting edge number is the totality of cutting edges involved in the cutting process. Kinematic methods combine the effects of the kinematics of the process with the statically determined grain distribution for the specification of mikrokinematics at the single grain, that is, for the determination of cutting parameters [3], [8]. **Figure 3** detaches various methods to determining the topography of grinding wheels.

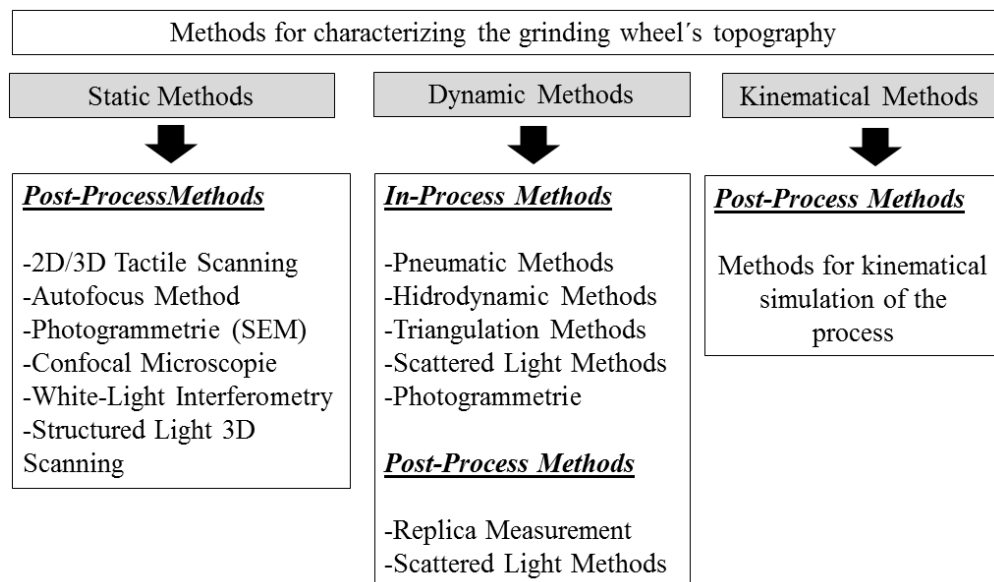


Figure 3: Methods for characterizing the grinding wheel's topography. Adapted and based on [3], [8], [9].

All the approaches mentioned above have certain advantages and disadvantages for the topography determination. Generally, the static methods and the post-process dynamic methods enable high defined surface topographies which lead to important applications for scientific issues. The high time-consuming procedures related to these methods represent their major drawbacks, thus preventing an application and integration in the industry. The in-process dynamic methods can be integrated in the production process but the significance of the results is mostly not sufficient to describe the surface topography of grinding wheels.

5. EXPERIMENTAL RIG

For running the scheduled experiments, an experimental rig based on a transducer fusion measuring technique has been developed. The transducer fusion measuring technique employs the acquisitions of both force and AE signals for extracting useful information about the topography of the fused oxide aluminium grinding wheel under investigation. The experiments are divided into two main procedures for characterizing the topography of the grinding wheel: a) Scratch Experiments and b) AE Tactile Scanning Experiments. When conducting the Scratch Experiments, only the monitoring of the grinding cutting force is put into practice (**Figure 4, dashed lines**) whereas during the AE Tactile Scanning Experiments only the measurement of AE signals is carried out (**Figure 4, continuous lines**). **Figure 4** schematically shows the signal chain in the experimental rig and the main devices that have been employed.

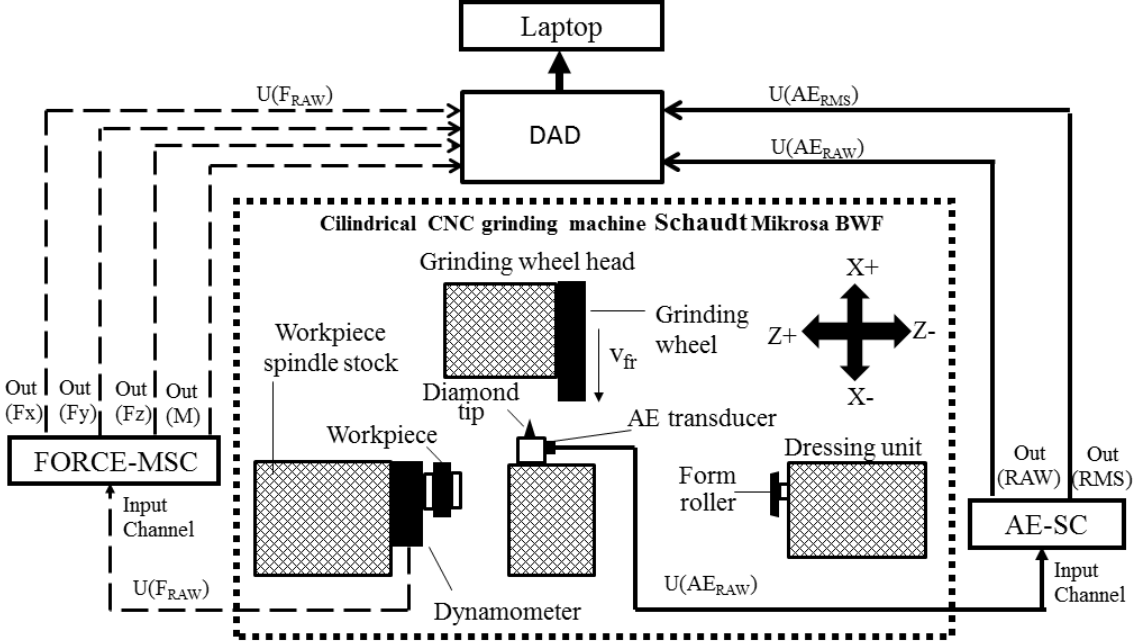


Figure 4: Experimental rig.

During the Scratch Experiments, the acquisition of the cutting force signals was implemented by using a dynamometer mounted in the workpiece's spindle stock. Therefore the components of the grinding cutting force (F_x , F_y , F_z , M) are measured by the dynamometer, converted to the voltage domain and sent via cable to its multichannel signal conditioner (Force-MSC), in order to proceed the signal conditioning of the analog voltage signals. After conditioning the analog signals (through signal amplification, and signal low-pass filtering), the output analog voltage signals are connected to the input channels of the data acquisition device (DAD) aiming at the signal digitization. Each output channel in the

Force-MSC has an analog low-pass filter which presents a cutoff frequency $f_c = 1$ kHz. Therefore the output analog voltage signals are digitized by using a sampling rate $f_s = 15,6$ kS/s in order to avoid aliasing effect (Shannon theorem). The digitized signals are afterwards transferred to a laptop (via USB cable) for data storage and signal post-processing of the main components of the grinding process (F_x , F_y , F_z , and M), by means of a developed algorithm in computational language.

For the AE Tactile Scanning Experiments, the AE signals are acquired by means of an AE-transducer which is mounted on the dressing support attached to the tailstock of the grinding machine. The AE_{RAW} signals are captured by the AE-transducer and then sent to the AE signal conditioner (AE-SC) through appropriate cable for signal processing (amplification, band-pass filtering, low-pass filtering and analog RMS conversion). Two AE-signal bandwidths (B) were separately investigated: a) $B_1 = (1 \text{ kHz up to } 100 \text{ kHz})$ and b) $B_2 = (1 \text{ kHz up to } 200 \text{ kHz})$. The bottom limits of both B_1 and B_2 are based on the constructive characteristics of the AE-transducer and on the electric circuit of the AE-SC, whereas the upper limits of both frequency bandwidths are determined by the selection of the cutoff frequencies (f_c) of the analog low-pass filters.

After signal conditioning the analog voltage signal, both the analog AE_{RAW} signal and the analog AE_{RMS} signal are transferred to the DAD for signal sampling and digitization. For selecting the suitable sampling frequencies, a laptop with a developed algorithm in a computational programming language is employed. The sampling frequencies used for digitizing either B_1 or B_2 were $f_{s1} = 200$ kS/s and $f_{s2} = 400$ kS/s, respectively, thus avoiding aliasing effect in the digitized AE signals. Besides on-line signal digitization, the developed algorithm also allows additional signal processing analysis for the in-process characterization of the grinding wheel's topography. The digitized signals are then sent to the laptop (via USB cable) aiming at signal monitoring, data storage and signal in-process evaluation, by using the same computational algorithm.

6. EXPERIMENTAL PROCEDURE

The experiments for characterizing the topography of the conventional grinding wheel have been divided into two distinct procedures: a) Scratch Experiments (Post-Process measurement Dynamic Method) and b) AE Tactile Scanning Experiments (In-Process measurement Dynamic Method).

The first procedure consists in plunge grinding a cylindrical workpiece (material: hardened steel alloy 100Cr6; initial diameter = 88,5 mm; width = 25 mm) by using a predefined rotational ratio of (1:5) between the investigated grinding wheel (diameter: 472 mm; width = 30 mm; grain material: fused aluminium oxide; bond material: ceramic; average grain size: 185 μm ,) and the workpiece. During the Scratch Experiments the grinding wheel's cutting speed is set at $v_s = 30$ m/s ($n_s = 1212 \text{ s}^{-1}$) and the number of workpiece revolutions is selected at $n_w = 262,6 \text{ s}^{-1}$, thus affording to the predefined rotational ratio.

The grinding wheel plunges against the workpiece's surface with a constant specific material removal rate ($Q'_w = 6 \text{ mm}^3/\text{mm}\cdot\text{s}$) and immediately reverses its plunge movement after reaching a predefined final diameter on the workpiece ($d_{w,final} = 87$ mm). Such reverse movement occurs without a spark out time, in order to scratch the actual topography of the grinding wheel on the workpiece. As the hardness of the workpiece is considerably high (860 HV), the plunge movement of the grinding wheel is divided into 5 incremental steps.

Each plunge movement of the grinding wheel against the workpiece grinds a constant specific material removal of $V'_w = 40 \text{ mm}^3/\text{mm}$, thus leading to a total specific material removal of $V'_{w,TOTAL} = 200 \text{ mm}^3/\text{mm}$ for each ground workpiece. During the plunge movement of the grinding wheel, the grinding cutting forces components (F_x , F_y , F_z) and the

grinding moment (M) are on-line monitored and the signals are saved in the laptop aiming at the post-processing of the normal force (F_n), and the tangential force (F_t). After plunge grinding, the topographical characteristic of the grinding wheel is analyzed by evaluating the effective roughness of the grinding wheel, (parameter R_{ts}), which is estimated through the measurement of the average roughness parameter R_a on the workpiece's periphery. As the proposed rotational ratio corresponds to 1:5 (one complete rotation of the grinding wheel for each 1/5 rotation of the workpiece) the grinding wheel's topography is represented 5 times over the periphery of the ground workpiece. By measuring the roughness parameter R_a in different angular positions incremented by 24° , it is possible to achieve average information about the topographic characteristic of the grinding wheel [3].

The second procedure consists in tactile scanning the topography of the grinding wheel by using the AE signals originated from the interferences (in the elastic deformation range) between the grinding wheel and a single diamond tip dressing tool. The topography of the grinding wheel is determined by evaluating the kinematical cutting edges which are on-line detected during the AE tactile scanning procedure. The proposed AE tactile scanning procedure is based on two main stages: stage-a) Determination of a reference position on the grinding wheel's periphery which serves as reference for the following stage; stage-b) Acquisition and in-process evaluation of AE_{RAW} signals derived from interferences between the grinding wheel and the diamond tip in the elastic deformation range.

6.1 Defining the Reference Position on the Grinding Wheel's Periphery (Stage-a)

The definition of a reference position on the grinding wheel's periphery plays an important role on the efficiency of the proposed AE tactile scanning procedure, as the interferences against the grinding wheel's topography and the diamond tip (during stage-b) occur in a range of a $1 \mu\text{m}$. Therefore, this procedure must be carried out as precisely as possible and involves distinct steps:

The first step consist in finding the first contact between the grinding wheel and the diamond tip by manually rotating the grinding wheel ($v_s \approx 5 \text{ m/s}$) and at the same time slowly infeed moving it ($v_{fr} \approx 2 \text{ mm/min}$) against the diamond tip. The infeed movement of the grinding wheel is also manually controlled. During the movement of the grinding wheel against the diamond tip, the AE signals are on-line monitored. When the first contact occurs, a burst-like AE signal is visualized on the laptop's screen, and the manually infeed movement is stopped. The X coordinate is saved for the second step.

In the second step, the grinding wheel is set to rotate with the same cutting speed used for grinding the workpiece during the Scratch Experiments ($v_s = 30 \text{ m/s}$). The grinding wheel moves against the diamond tip down to $X_2 = X_1 + 0,06 \text{ mm}$ (allowance distance). After reaching X_2 , the first contact is found by infeed moving the grinding wheel with stepwise increments of $1 \mu\text{m}$ and the simultaneously observation of the AE signals in the laptop's screen. Such increments are manually commanded by the operator until the first contact (AE burst-type signal) is found (coordinate X_3) which is stored in the NC command of the grinding machine and serves as reference for the increments used at the stage-b.

6.2 Acquisition and In-Process Evaluation of AE_{RAW} signals (Stage-b)

In contrast to the stage-a, all the relative movements between grinding wheel and the diamond tip at stage-b are NC controlled. After defining the reference position on the grinding wheel's periphery (as proposed at stage-a), the grinding wheel is set to $v_s = 30 \text{ m/s}$. Next, the diamond tip is positioned in the same Z coordinate which has been previously adopted for determining the reference position on the grinding wheel's periphery. The grinding wheel is

then guided towards X_2 (allowance distance from the diamond tip) with a fast infeed movement in the X direction while maintaining the same Z coordinate during this movement ($Z = \text{constant}$). At the position X_2 , the infeed velocity is decreased to $v_{fr} = 0,5 \text{ mm/min}$ and the grinding wheel moves slowly against the diamond tip down to $1 \mu\text{m}$ in relation to the reference position X_3 ($a_{e,scan} = 1 \mu\text{m}$), which was found at stage-a). Such interference situations in the elastic deformation range of the grinding wheel and therefore does not alter the topography of the grinding wheel during the experiments.

After reaching $a_{e,scan} = 1 \mu\text{m}$, the grinding wheel stops its infeed movement, and moves axially in a total scanning length, $L_{scan} = 10 \text{ mm}$ by using a constant scanning velocity, $v_{f,scan} = 120 \text{ mm/min}$. The AE_{RAW} signals originated in such interference conditions present the duration of $t_{scan} = 5 \text{ s}$ and are recognized by the AE-transducer. Subsequently to the AE_{RAW} acquisition in the course of L_{scan} , the grinding wheel moves backwards to the save distance from the diamond tip. Then, based on the AE_{RAW} which is acquired during t_{scan} , the computational algorithm evaluates in-process both a time domain and a frequency domain analysis output for characterizing the grinding wheel's topography.

The output derived from the time domain analysis consists in a number directly related to the actual condition of the grinding wheel's topography. This number is associated to the total number of oversteps of the AE_{RAW} signal (during t_{map}), in relation to a fixed predefined threshold. The predefined threshold situates a certain level above the maximum value of the AE_{RAW} ground noise signal, in order to be not influenced by occasional disturbances in the AE_{RAW} signal and also to allow expressing useful information about the grinding wheel's topography. On the other hand, the output from the frequency domain analysis comprises the assessment of the AE_{RAW} spectrum for both bandwidths (B1 and B2, see Section 5: Experimental Rig) under investigation.

7. EXPERIMENTAL PLANNING

The conducted experiments in the scope of the present research were planned as proposed in Figure 5. The arrow at the right side of Figure 5 illustrates the progress of the experiments series over time.

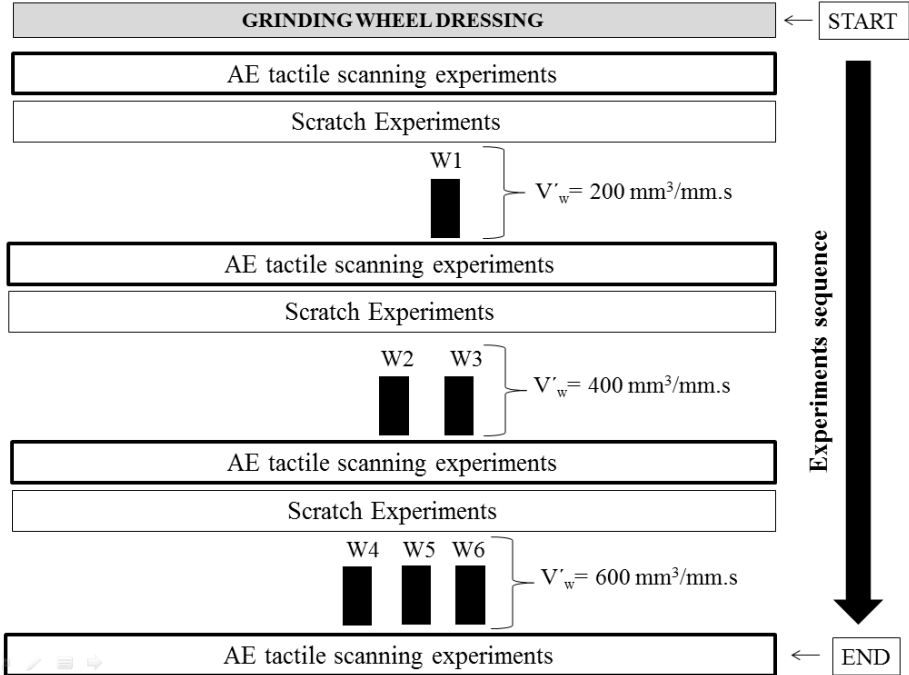


Figure 5: Experimental planning.

The experiments series begin by firstly dressing the grinding wheel aiming at to afford a flat initial topography on the grinding wheel's surface. For dressing the grinding wheel a form roller (diameter $d_R = 120$ mm, flat profile, active width $b_d = 0,6$ mm) presenting a one-sided diamond coating, has been used. The dressing roller circumferential speed (v_R) was set at $v_R = 17,25$ m/s and its axial dressing feed rate was $v_{fad} = 720$ mm/min (12 mm/s). The grinding wheel circumferential speed during dressing (v_{sd}) was adjusted at the same value of its cutting velocity (v_s) used during grinding, so that, $v_{sd} = v_s = 30$ m/s, thus resulting in a dressing speed ratio of $q_d = -0,575$ where the negative value refers to up dressing. As the active width of the dressing tool is $b_d = 0,6$ mm and the dressing feed per grinding wheel revolution was set at $f_{ad} = 0,6$ mm/rot, the resulting overlap ratio corresponds to $U_d = 1$. A total of 5 dressing passes are repeated sequentially in order to eliminate eventual disturbances which arise from the grinding wheel's surface. Each dressing pass is on-line monitored with the support of the AE-SC and the laptop.

The AE Tactile Scanning Experiments are carried out after dressing the grinding wheel aiming at to evaluate an initial condition of the grinding wheel's topography. Additionally, these experiments occur both between the Scratch Experiments and at the end of the experiments series, in order to in-process characterizing the induced changes on the grinding wheel's topography. The actual state of the grinding wheel's topography is determined by using a developed signal conditioning procedure which allows extracting in-process information about the grinding wheel's topography both in time-domain as well as in the frequency-domain signal analysis.

The time-domain output of the proposed signal analysis consists in a number, which represents the total oversteps of the AE_{RAW} signal in relation to a fixed predefined threshold lying above the AE_{RAW} ground signal. This number is obtained in-process and instantaneously visualized on the laptop's screen (when pushing the stop button of the acquisition program application) after finishing the AE Scanning experiment. Besides the threshold, additional factors that also directly influence the time-domain output are the type of the AE signal and the sampling frequency (f_s). These 3 factors were varied in 2 levels (high \uparrow , and low \downarrow) whose magnitudes were defined previously to the experiments series. **Table 1** show the main experimental runs which have been investigated during the AE Tactile Scanning Experiments. Line "a" illustrates the experimental situation in which the factor A "Type of Signal" is set at its high level (AE_{RAW}) whereas both Factor B "Sampling Frequency" and the Factor C "Threshold", are set at their lower levels (200 kS/s, and minimal threshold, respectively). The levels of the factor C "Threshold", depend heavily on the type of the AE signal as well as on the ground noise of the AE signal. In order to avoid that occasional disturbances in the AE signal erroneously overstep the selected value of threshold, the lower level of factor C "Threshold" (\downarrow) lies 0,03 V above the maximum value of the AE ground noise. On the other hand, the high level of the factor C "Threshold" (\uparrow) is always set at 0,05V above the lower level of factor C "Threshold". Therefore, casual offsets in the AE signal and signal disturbances do not affect the proposed procedure over the experiments series. Each experimental run shown in **Table 1** has been repeated 3 times in order to get an average representative value along the experiments, so that a total of 12 AE signals are obtained for each stage of the AE Tactile Scanning Experiments. Therefore, a total of 48 AE signals are sampled at the end of the scheduled AE Tactile Scanning Experiments (bottom line in **Figure 5**).

MAIN FACTORS AND LEVELS			
Experimental runs	FACTOR A= Type of AE Signal	FACTOR B= f_s	FACTOR C= Threshold
	$\uparrow = AE_{RAW}$ $\downarrow = AE_{RMS}$	$\uparrow = 400$ kS/s $\downarrow = 200$ kS/s	$\uparrow = HIGH$ (V) $\downarrow = LOW$ (V)
a	↑	↓	↓
b	↓	↑	↓
c	↓	↓	↑
abc	↑	↑	↑

Table 1: Experimental runs during AE Tactile Scanning Experiments.

The frequency-domain output from the proposed signal analysis consists in a chart which shows the evaluation of the AE spectrum based on the AE_{RAW} signals. This chart allows obtaining complementary information about the changes on the grinding wheel's topography along the experiments series when increasing V'_w . Such AE spectrum evaluation is also achieved in-process and instantaneously visualized on the laptop's screen (when pushing the stop button of the acquisition program application) after finishing the AE Tactile Scanning Experiment.

Along with the Scratch Experiments series, a total of 6 workpieces (W) have been ground accounting for a total specific material removal $V'_{w,total} = 1200$ mm³/mm. From the very beginning of the Scratch Experiments until the end, the amount of V'_w gradually increases in order to purposively wear the grinding wheel and change its topography.

8. RESULTS

This section presents the achieved results for both the Scratch Experiments and the AE Tactile Scanning Experiments. The Scratch Experiments results are based on the post-process measurements of both the cutting forces components and the grinding wheel surface roughness R_{ts} . The AE Tactile Scanning results are derived from the in-process measurement analysis in both time and frequency domain.

8.1 Scratch Experiments Results

The first results derived from the Scratch Experiments consist in the evaluation of the main components of the grinding force (F_n and F_t) by processing the cutting force signals (F_x , F_y , F_z and M) acquired during the grinding process. Such evaluation occurs after finishing the Scratch Experiments, that is, it represents a post-process evaluation. In order to allow an interpretation independent from the grinding wheel's width, both F_n and F_t are divided by the effective width of the grinding wheel, thus leading to the evaluation of the specific grinding force components, F'_n and F'_t , respectively. **Figure 6** shows the evaluated values of F'_n and F'_t over V'_w along the Scratch Experiments series.

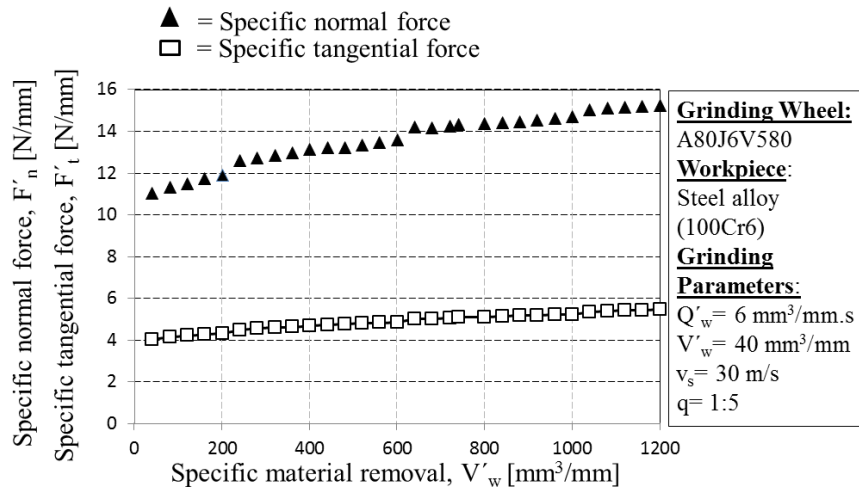


Figure 6: Specific grinding cutting force components (F'_n, F'_t) x V'_w .

Each plotted point in **Figure 6** represents the magnitude of the specific grinding cutting force component during the plunge movement of the grinding wheel against the workpiece's surface. It can be seen that both F'_n as well as F'_t increase with gradually enlarged values of V'_w . As all the grinding process input parameters are kept constant during the Scratch Experiments (with the exception of V'_w), the increasing trend observed in **Figure 6** is associated with a growth of N_{kin} (kinematical cutting edges) for the investigated grinding wheel. Further significant results from the Scratch Experiments have been obtained by correlating the actual grinding wheel surface roughness (R_{ts}), with V'_w , **Figure 7**.

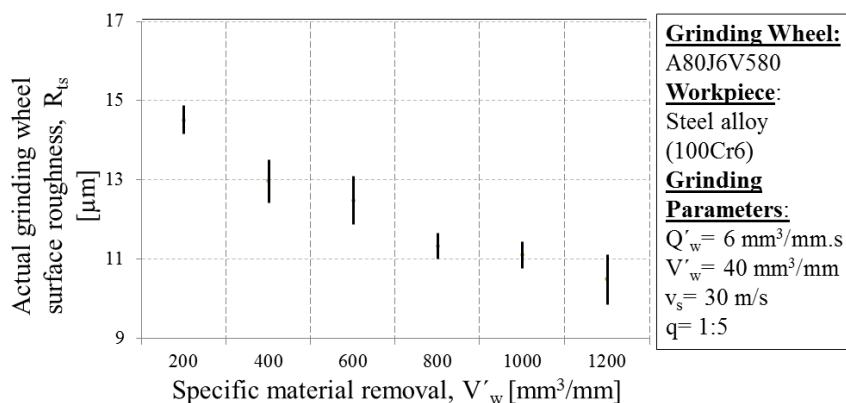


Figure 7: Actual grinding wheel surface roughness R_{ts} , x V'_w .

The actual grinding wheel surface roughness R_{ts} is estimated by indirectly measuring the surface roughness of the ground workpiece with the roughness parameter R_a . Therefore, each measuring result plotted in **Figure 7** corresponds to the mean value based on 12 R_a roughness measurements extracted from the workpiece's surface in predefined positions. The vertical straight lines in **Figure 7** correspond to the spread of the R_a measurements results (mean's variance). It is possible to observe that R_{ts} decreases with gradually enlarged values of V'_w , thus indicating that more kinematic cutting edges are taking part in the grinding process. This tendency can also be explained by the fact that higher values of N_{kin} reduce the chip thickness (h_{cu}) what in turn leads to smaller values of R_{ts} evaluated on the workpiece. Therefore, such trend of the grinding wheel's topography leads to the assumption that N_{kin} increases with higher values of V'_w which also correlates with the previous cutting force's analysis.

8.2 AE Tactile Scanning Experiments' Results

The results regarding the AE Tactile Scanning Experiments are divided into two complementary analyses: a) time domain analysis and, b) frequency domain analysis. Either analyses allow extracting in-process information about the actual topography of the investigated grinding wheel. In the time domain analysis, the topography of the grinding wheel is characterized by a number, which consists of the total amount of AE oversteps in relation to a fixed predefined threshold. On the other hand, in the frequency domain analysis the topography of the grinding wheel is characterized by specific changes in the AE spectrum. The processing of both the time and frequency domain analysis is instantaneously achieved in-process, immediately after finishing the AE Tactile Scanning Experiment. **Figure 8** shows the results derived from the time domain analysis for the experimental runs "a", "b", "c", and "abc".

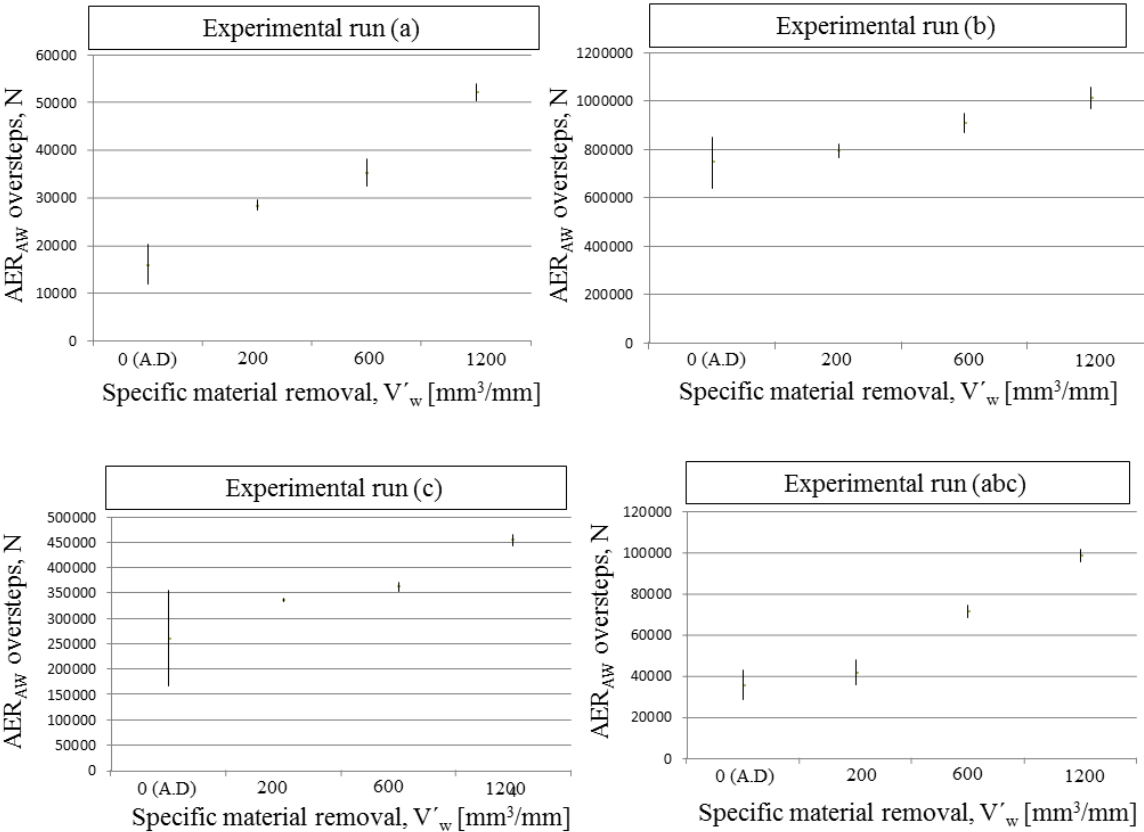


Figure 8: In-process time domain analysis of AE signals.

The plotted graphs in **Figure 8** represent the mean value (sample size, $n= 3$) of the AER_{RAW} oversteps N , as well as the mean's variance of N obtained in-process by employing the time domain analysis. The results plotted at the left portion of all graphs show the initial condition of the grinding wheel after dressing (A.D), before grinding the workpiece ($V'_w= 0$ mm³/mm). The graphs show a similar trend for all the four considered experimental runs which have been tested during the experiments. The experimental combinations show a remarkable growth in the number of N for increasing values of V'_w . This trend is quite pronounced when comparing the values of N both after grinding $V'_w= 200$ mm³/mm and $V'_w= 1200$ mm³/mm. Such results correlate with those obtained from the Scratch Experiments results, thus also indicating that the topography of the grinding wheel tends to present higher values of N_{kin} when increasing V'_w . The experimental conditions "b", and "c", seem to be

reliable to recognizing different grinding wheel's topographies associated with distinct wear of the grinding wheel (for example between $V'_w = 200 \text{ mm}^3/\text{mm}$ and $V'_w = 1200 \text{ mm}^3/\text{mm}$), whereas the experimental runs "a" and "abc" show a better efficiency in recognizing small differences in the grinding wheel's topography. For the experimental run "c", an unexpected spread of the mean value of N after grinding $V'_w = 200 \text{ mm}^3/\text{mm}$ has been observed, which should be better explained through additional experimentation. The results achieved in all the four experimental runs, indicate that the proposed time domain analysis is suitable for recognizing distinct topographies of the grinding wheel in-process.

In order to afford complementary information about the changes in the grinding wheel's topography occurring along the experiments, the frequency domain analysis is also carried out in-process. **Figure 9** shows the results derived from the frequency domain analysis for the experimental runs "a", "abc", which include the use of AE_{RAW} signals.

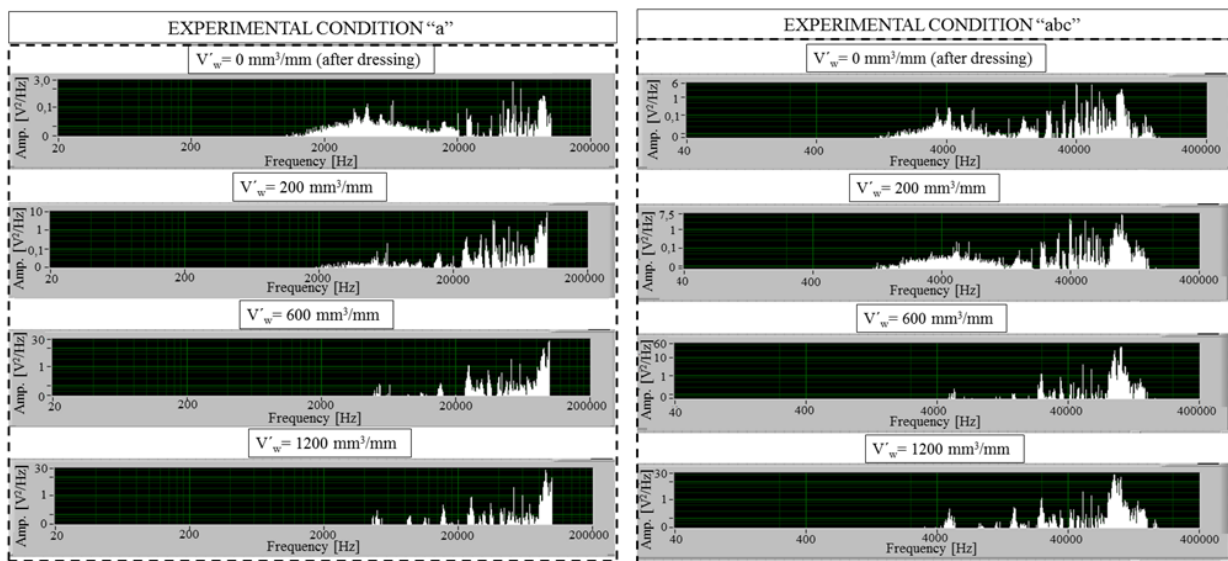


Figure 9: In-process frequency domain analysis of AE_{RAW} signals.

Figure 9 shows the frequency domain results evaluated from eight AE_{RAW} signals associated with the experimental runs "a" and "abc" (see **Table 1**). The graphs at the upper part in this figure are obtained right after the dressing process, whereas the other graphs are evaluated in-process for each specific stage of the experiments series and related to a predefined specific material removal V'_w ground in the workpiece.

When observing the graphs derived from the experimental run "a" (**Figure 9**, left side), the maximum frequency content consists of $f_{max} = 100 \text{ kHz}$, as in this experimental run the AE_{RAW} signals are digitized by using a sampling frequency of $f_s = 200 \text{ kHz}$. Such value is twice as high as the selected cutoff frequency of the analog low-pass filter ($f_{cutoff} = 100 \text{ kHz}$) installed in the AE-SC. On the other hand, the graphs derived from the experimental run "abc" present a broader frequency content which can reach up to $f_{max} = 200 \text{ kHz}$ due to the use of an analog low-pass filter which comprises a higher value of the cutoff frequency ($f_{cutoff} = 200 \text{ kHz}$). Therefore these signals have been sampled with $f_s = 400 \text{ kHz}$.

For both the experimental run "a", and experimental run "abc", the frequency domain signals present a similar trend as V'_w gets higher along the experiments series. This trend is characterized by a gradually shift in the AE spectrum which changes from a highly broad spectrum at $V'_w = 0 \text{ mm}^3/\text{mm}$ (after dressing) to a quite better defined spectrum (and less influenced by the lower frequencies) after plunge grinding $V'_w = 1200 \text{ mm}^3/\text{mm}$. Such tendency in the AE spectrum can be attributed to the increase of N_{kin} taking effect on the

grinding wheel's topography as V'_w gets higher, while also correlating with the previous results derived from both the Scratch Experiments, as well as the time domain analysis.

When comparing the frequency domain results plotted for the experimental run "a" and the experimental run "abc" in the same value of V'_w , it is possible to realize that substantial information is gained by using $f_s = 400$ KS/s. This information gain is mainly significant in the AE frequency range from 100 kHz up to 200 kHz.

9. CONCLUSIONS

The presented results achieved in the scope of the present research show that the proposed AE quick-test method is feasible to characterizing the grinding wheel's topography in-process by extracting quantified information from the grinding wheel's topography features. This is achieved with the same grinding setup and experimental rig, without the need for implementing a post-analysis out of the grinding process. Such versatility presented by the proposed AE quick-test method consists in the first main advantage of such procedure. Furthermore, when comparing the presented AE quick-test method's results with other grinding wheel's characterization methods available in the literature, the proposed method permits to evaluate quantified in-process information related to the topography of the grinding wheel by using customary grinding wheel cutting speeds usually employed in the industrial praxis (for example, $v_s = 30$ m/s). Such information is obtained without requiring decelerating the grinding wheel cutting speed, thus representing more significant information related to the grinding process. In order to afford reliable information about the changes in the grinding wheel's topography along the experiments, the AE quick-test method permits to conduct both in-process time domain and in-process frequency domain analysis.

The results derived from the time domain analysis follow a very similar trend along with the increasing values of V'_w and maintain a consistent tendency for all the four investigated experimental runs ("a", "b", "c", and "abc"). By observing the results from the time domain analysis, a significant difference appears between the number of AE oversteps (N) associated with $V'_w = 0$ mm³/mm (after dressing) and those achieved after grinding the specific amount of material $V'_w = 1200$ mm³/mm, for all the experimental runs. These results are associated with a growth of N_{kin} over V'_w , as also indicated in the results extracted from the Scratch Experiments. The experimental runs "a" and "abc" present higher sensitivity than the experimental conditions "b" and "c", due to the high slope verified in their $N \times V'_w$ graphs. Additionally, the repeatability verified in the results obtained from the experimental conditions "a" and "abc" are suitable for characterizing distinct grinding wheel's topographies. Therefore, the conditions "a" and "abc" are the most optimized conditions for in-process recognizing both close differences in the grinding wheel's topography (for example verified between $V'_w = 200$ mm³/mm and $V'_w = 600$ mm³/mm) and totally dissimilar conditions in the grinding wheel's topography (for example verified between $V'_w = 200$ mm³/mm and $V'_w = 1200$ mm³/mm).

The frequency domain results investigated in the optimized experimental conditions "a" and "abc" show a very similar tendency in their AE_{RAW} spectrums when increasing the amount of V'_w along the experiments. Either experimental conditions show a noticeable change towards a high frequency concentration in the evaluated AE_{RAW} spectrum for enlarged values of V'_w , thus permitting to distinguish in-process both the initial condition and the final condition of the grinding wheel's topography. The changes verified in the AE_{RAW} spectrum can also be associated with a growth of N_{kin} during the experiments which correlates with the results shown in the time domain analysis and the results extracted from the Scratch Experiments. The spectrum content derived from the AE_{RAW} signals at the experimental

condition “abc” allow getting additional information about the grinding wheel’s topography, especially in the frequency range from 100 kHz up to 200 kHz without aliasing effect.

The combined use of both the time domain and the frequency domain results obtained in-process by means of the AE quick-test method allows identifying both small changes in the grinding wheel’s topography and totally dissimilar conditions on the surface of the grinding wheel. As the results derived from both the time and frequency analysis correlate with those results derived from the Scratch Experiments, the proposed AE quick-test method can be validated for further utilization in the industrial and academia praxis.

10. REFERENCES

- [1] H. K. Tonshoff, T. Friemuth, J. C. Becker, “**Process Monitoring in Grinding**”, Institute of Production Engineering and Machine Tools, University of Hannover, Germany.
- [2] D.E. Lee, I. Hwang, C.M.O. Valente, J.F.G. Oliveira, D.A. Dornfeld, ”**Precision Manufacturing Process Monitoring with Acoustic Emission**”, International Journal of Machine Tools and Manufacture, 2006.
- [3] W. König, “**Fertigungsverfahren Band 2: Schleifen, Honen, Läppen**”, Düsseldorf, 1989.
- [4] W. Klufft “**Process Monitor GD 200, G200 und D200**”, Aachen, 1989, Germany.
- [5] A. Hassui et al. “**Experimental Evaluation on Grinding Wheel Wear through Vibration and Acoustic Emission**”, Unicamp, São Paulo, Brasil, 1998.
- [6] B. Karpuschewski, “**Sensoren zur Prozessüberwachung beim Spanen**”, Werkzeugmaschinenlabor (WZL), Aachen, Germany, 2001.
- [7] D.I. Marinescu, W.B. Rowe, B. Dimitrov, and I. Inasaki, “**Tribology of Abrasive Machining Processes**”, Willian Andrew publishing, USA, 2004.
- [8] D.I. Marinescu, M. Hitchiner, E. Uhlmann, “**Handbook of Machining with Grinding Wheels**”, London. 2007.
- [9] M. Duscha, “**Erfassung und Charakterisierung der Schleifscheibentopographie für die Anwendungsgerechte Prozessauslegung**”. Diamond Business, 1/2009.
- [10] W. Hundt, F. Kuster, F. Rehsteiner, “**Model-Based AE Monitoring of the Grinding Process**“, Anals of the CIRP, vol. 46, IWF, ETH Zürich, 1997.

11. ACKNOWLEDGMENTS

The results presented in this paper are part of the author’s PhD research work which is being carried out in the context of the CAPES/DFG international cooperation program BRAGECRIM (Brazilian - German Collaborative Research Initiative on Manufacturing Technology) and developed in a partnership between the LMP (*Laboratório de Mecânica de Precisão*) at the UFSC (Federal University of Santa Catarina), in Florianópolis, Brazil, and the IWF (*Institut für Werkzeugmaschinen und Fabrikbetrieb*) at the TU-Berlin (*Technische Universität Berlin*), in Berlin, Germany.